

20. C. J. F. Ter Braak, *Technical Report LWA-88-02* (Institute of Applied Computer Science, Wageningen, Netherlands, 1988).
21. J. F. Talling, *Int. Rev. Ges. Hydrobiol.* **51**, 545 (1966); P. Kilham, S. S. Kilham, R. E. Hecky, *Limnol. Oceanogr.* **31**, 1169 (1986).
22. D. Meese *et al.*, *U.S. Army Cold Reg. Res. Eng. Lab. Publ. SR94-01* (1994).
23. P. M. Grootes *et al.*, *Eos* **75**, 225 (1994); P. A. Mayewski *et al.*, *Science* **272**, 1636 (1996).
24. P. A. Mayewski *et al.*, *Science* **263**, 1747 (1994).
25. T. M. L. Wigley, in *Global Changes of the Past*, R. S. Bradley, Ed. (University Consortium of Atmospheric Research, Office for Interdisciplinary Earth Studies, Boulder, CO, 1989), pp. 83–101.
26. R. B. Alley *et al.*, *Geology*, in press.
27. R. B. Owen, J. W. Barthelme, R. W. Renaut, A. Vincens, *Nature* **298**, 523 (1982); K. W. Butzer, G. L. Isaac, J. L. Richardson, C. Washbourn-Kamau, *Science* **175**, 1069 (1972).
28. J. Maley, *Quat. Res.* **18**, 1 (1982).
29. P. A. Mayewski *et al.*, *Antarct. Res. Ser.* **67**, 33 (1995).
30. D. A. Fisher, R. M. Koerner, N. Reeth, *Holocene* **5**, 19 (1995); X. Feng and S. Epstein, *Science* **265**, 1079 (1994); R. W. Mathewes and L. E. Heusser, *Can. J. Bot.* **59**, 707 (1981).
31. P. Blanchon and J. Shaw, *Geology* **23**, 4 (1995); J. T. Overpeck *et al.*, *Nature* **338**, 553 (1989).
32. E. van Campo and F. Gasse, *Quat. Res.* **39**, 300 (1993); A. Frumkin *et al.*, *Holocene* **1**, 191 (1991); R. A. Bryson and A. M. Swain, *Quat. Res.* **16**, 135 (1981).
33. M. Stuiver and T. F. Brauzanias, *Nature* **338**, 405 (1989).
34. P. D. Tyson and J. A. Lindesay, *Holocene* **2**, 271 (1992); T. C. Partridge, *Mem. Soc. Geol. France* **167**, 73 (1995).
35. We thank the NSF for financial support for the TD ice core project; the Polar Ice Coring Office (University of Alaska) drillers, notably D. Giles; the Antarctic Support Associates personnel for camp support and logistics; Squadron VXE6 and the New York Air National Guard (TAG 109) for air support; P. Grootes, E. Steig, M. Stuiver, D. Morse, E. Waddington, and other colleagues at the University of Washington for organizing, collecting, and dating the TD ice core; and K. Beuning, B. Cumming, S. Grimm, T. Johnson, K. Laird, D. Livingstone, M. Martin, L. Meeker, Paul Smith's College, and J. Smol for support in the Lake Victoria project.

25 February 1997; accepted 25 April 1997

Giant Planet Formation by Gravitational Instability

Alan P. Boss

The recent discoveries of extrasolar giant planets, coupled with refined models of the compositions of Jupiter and Saturn, prompt a reexamination of theories of giant planet formation. An alternative to the favored core accretion hypothesis is examined here; gravitational instability in the outer solar nebula leading to giant planet formation. Three-dimensional hydrodynamic calculations of protoplanetary disks show that giant gaseous protoplanets can form with locally isothermal or adiabatic disk thermodynamics. Gravitational instability appears to be capable of forming giant planets with modest cores of ice and rock faster than the core accretion mechanism can.

The discovery of extrasolar giant planets (1–5) presents theorists with the challenge of trying to understand the formation of these planets within the context of the generally accepted core accretion model for the formation of the solar system's giant planets. The core accretion model envisions the formation of cores of roughly $10 M_{\oplus}$ (M_{\oplus} = the mass of Earth) through planetesimal collisions, followed by rapid accretion of gas from the solar nebula (6). However, the core accretion model suffers from the fact that the time needed to assemble the $10 M_{\oplus}$ cores, which is on the order of 10^6 years in the most optimistic scenario (7), lies in the middle of the range of ages ($\sim 10^5$ to $\sim 10^7$ years) at which young solar-type stars lose their gaseous disks (8). If the disk gas has already dissipated by the time that $10 M_{\oplus}$ cores form, then Uranus-like planets would result, rather than Jupiter-like planets, a fate that led to some understandable pessimism about the frequency of occurrence of extrasolar giant planets (9).

The detection of a number of extrasolar planets with minimum masses ranging from 0.5 to $4 M_J$ ($M_J = 318 M_{\oplus}$ = the mass of Jupiter) has removed much of the concern that giant planets might be rare in our

galaxy. For detection by the radial velocity technique, the planet's mass will be considerably larger than the minimum if the planet's orbit is nearly in the plane of the sky. The suspected giant planets orbiting 47 Ursae Majoris (2), Lalande 21185 (3), and 16 Cygni B (4) have semimajor axes of 2 to 7 astronomical units (AU) ($1 \text{ AU} = 1.5 \times 10^{13} \text{ cm}$ = the distance from Earth to the sun), and have minimum masses of 1.5 to $2.4 M_J$; Lalande 21185's astrometrically detected planet is fixed in mass at $1.5 M_J$. The core accretion model may be unable to produce giant planets more massive than about $1 M_J$ if the growing planet's gravity induces a gap in the surrounding disk (10). In addition, suspected brown dwarf stars (stars with $M < 80 M_J$) have also been found in orbit around nearby stars (11), with minimum masses as small as $6.6 M_J$ (12), possibly blurring any mass-based distinction between planets and brown dwarf stars (13).

The core accretion model won favor largely because of its ability to explain the similarity of the masses of the ice and rock cores inferred for Jupiter, Saturn, Uranus, and Neptune through the prediction (14) of the existence of a single critical core mass ($\sim 10 M_{\oplus}$) that would trigger gas accretion throughout the solar nebula. However, recent models of the interior

structure of Jupiter and Saturn (15) have concluded that their ice and rock core masses are smaller than had previously been thought likely: 3 to $10 M_{\oplus}$ for Jupiter and 1 to $13 M_{\oplus}$ for Saturn, as compared with the older estimates (16) of 10 to $30 M_{\oplus}$ for Jupiter and 15 to $25 M_{\oplus}$ for Saturn. If the lower estimates are accurate, then much of the attraction of the core accretion theory would be lost because lower mass cores might not be able to trigger gas accretion.

For these and other reasons (7), it seems prudent to reevaluate the possible mechanisms for giant planet formation. One hypothesis is the gravitational instability mechanism (17), in which the solar nebula breaks up through its own self-gravity into clumps of gas and dust, termed giant gaseous protoplanets (GGPPs), which then contract and collapse to form giant planets (18). The GGPP mechanism was discarded because of its failure to explain the large values and similarity of estimated core masses for both the giant and the outer planets (6, 16), but these problems may no longer exist.

Previous work on gravitational instabilities in disks had suggested that marginally unstable disks would evolve through the formation of spiral density waves (19), thereby avoiding GGPP formation, and that GGPPs could only occur if the disks were strongly unstable (20). GGPP formation also seemed to require that the instability proceed at a fixed temperature at a given orbital radius (that is, locally isothermal), in order to prevent thermal pressure from damping the growth of the perturbations (20).

In the process of calculating axisymmetric models of the temperature distribution in the solar nebula (21), the general trend arose of relatively hot (midplane temperature $T_m \sim 1000 \text{ K}$) regions inside a few AU, surrounded by relatively cold ($T_m \sim 100 \text{ K}$) outer regions. In disks with masses of $\sim 100 M_J$ inside 10 AU, the outer regions were dense enough to be

Department of Terrestrial Magnetism, Carnegie Institution of Washington, Washington, DC 20015–1305, USA.

marginally gravitationally unstable, according to Toomre's stability criterion (22). Such a situation might permit a "best of both worlds" scenario, in which the formation of the terrestrial planets occurred through collisional accumulation of solids in the hot inner nebula (23), while the giant planets formed rapidly ($\sim 10^3$ years) once the nebula becomes unstable through the growth of GGPPs in the cool outer nebula. The outer planets (Uranus and Neptune) would still need to form by the slow process of collisional accumulation, completing their growth well after the giant planets had formed and the nebular gas had been dissipated.

Because of their limitation to axisymmetry, the previous two-dimensional (2D) models (21) could not directly address the question of the outcome of any possible gravitational instability. Here a 3D hydrodynamics code is used to study GGPP formation in protoplanetary disks defined by the previous axisymmetric calculations. The gravitational hydrodynamics code has been used to study a variety of problems in protostellar collapse and protoplanetary disk evolution (24). The code solves the equations of hydrodynamics and the Poisson equation on a spherical coordinate grid and is second-order-accurate in space and time.

The GGPP instability depends on disk self-gravity overwhelming the thermal pressure inside the disk, so the assumed disk thermodynamics is critical. The 3D models start with the thermal structure of an axisymmetric disk with a mass of $\sim 140 M_J$ orbiting a star of one solar mass, as determined by the previous radiative hy-

drodynamic calculations (21). Because radiative transfer is prohibitively slow for these 3D models, the effects of disk thermodynamics were investigated by arbitrarily varying the outer disk temperature profile and by varying the effective adiabatic exponent (pressure P depends on density ρ as $P \propto \rho^\gamma$) from $\gamma = 1$ (isothermal) to $\gamma = 7/5$ (adiabatic for molecular hydrogen). These two values of γ should span the appropriate range for the solar nebula, with the larger value of γ implying higher temperatures and pressures and increased resistance to GGPP formation.

The active computational volume (number of grid points in each direction: $N_r = 51$, $N_\theta = 23$ in $\pi/2 \geq \theta \geq 0$, $N_\phi = 64$) extends from 1 to 10 AU, with boundary conditions at both 1 AU and 10 AU chosen to absorb velocity perturbations and at 10 AU to maintain constant density. The initial disk density is seeded with a nonaxisymmetric $\cos 2\phi$ perturbation (an $m = 2$ mode of amplitude $a_2 = 0.01$) and with random noise (modes $m = 1, 2, \dots, 16$ with $a_m \sim 0.001$), biasing the disks toward the formation of two-armed spiral structures. The rotation period at the inner edge of the disk is $P_i \approx 1$ year, and at the outer edge the rotation period is $P_o \approx 28$ years. With the locally isothermal or adiabatic assumptions, the disk models can be computed for many rotation periods of the outer disk, $\sim 15 P_o$, as is needed to follow the growth of nonaxisymmetry in marginally unstable disks.

The results of two models are presented here, one with locally isothermal ($\gamma = 1$; model LI) and one with locally adiabatic ($\gamma = 7/5$; model LA) thermodynamics. Model LI used the temperature profile computed

for the $135 M_J$ disk in (21), which approached $T_m \approx 100 \pm 50$ K in the outer disk. Model LA used the same temperature profile as model LI, except that the outer disk temperature (beyond 7.4 AU) was assumed to approach 50 K instead of 100 K. The outer disk temperatures are not as well constrained by the previous modeling as the inner disk temperatures are, and so this seemingly arbitrary change from 100 K to 50 K is roughly within the uncertainty of the previous models (21).

The initial disk models are characterized by their Toomre Q parameters (22). The inner regions of both disks are stable, with $Q \gg 1$, but Q drops to close to 1 around 7.5 AU in both models (Fig. 1). In model LI, Q hovers around the critical value of 1 beyond 7.5 AU, whereas in model LA Q drops below 1 to about 0.8 (Fig. 1). Other models (25) demonstrate that disks are unstable for a range of values of $Q \sim 1$, including Q values slightly higher than those of models LI and LA, so the precise values of Q chosen here are not crucial to the general outcome of the instability.

Both models evolved in a similar fashion despite their different adiabatic exponents. The initial bar-shaped perturbation rapidly wound up into a trailing two-arm spiral pattern, which underwent a prolonged period of steady growth. For the first several hundred years, the amplitude of the $m = 2$ mode grew roughly linearly with time. By the end of the simulations, the amplitudes of the $m = 1, 2, 3$, and 4 modes had all grown from ~ 0.001 (from 0.01 for $m = 2$) to the range 1.4 to 1.6, nearing saturation, with most of the

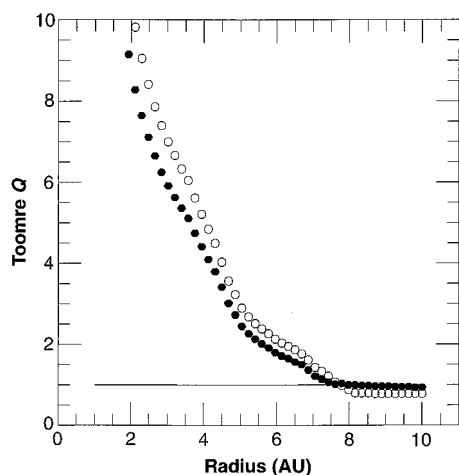


Fig. 1. Toomre Q stability parameter as a function of distance from the protostar in the locally isothermal model LI (filled symbols) and the locally adiabatic model LA (open symbols) at the start of the calculations. The horizontal line shows the critical value ($Q = 1$) for instability to the growth of nonaxisymmetric perturbations.

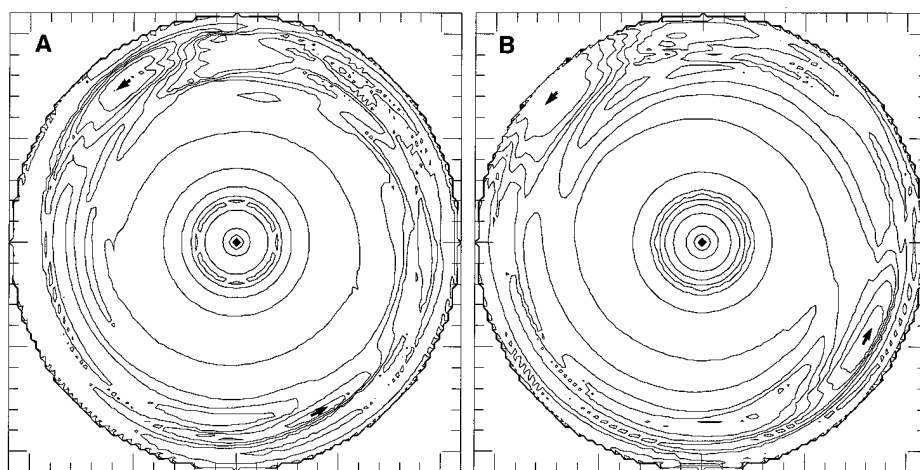


Fig. 2. Equatorial density contours (factors of 2) showing the outcome of the locally isothermal model LI (A) after 430 years and of the locally adiabatic model LA (B) after 550 years. Each disk forms two giant gaseous protoplanets (arrows denote their centers and directions of motion), though of unequal mass in both cases. Each GGPP is trailed by a low-density region and thin spiral arms. A solar-mass protostar lies at the center (diamond) of the disks. The region shown is 20 AU in diameter; jagged outer contours mark the outer edge of the spherical coordinate computational grid. The maximum density in both plots is $1 \times 10^{-8} \text{ g cm}^{-3}$.

growth of the $m \neq 2$ modes occurring in the last 200 years of the evolution.

The self-gravitational forces of the growing spiral density waves overwhelmed the thermal pressure in the disks, resulting in each disk breaking up into two GGPPs (Fig. 2). The maximum density in each GGPP was still increasing at the time when the calculations were stopped because the outcome was obvious—in model LI, the maximum GGPP density nearly doubled in the last 30 years. In both models, the GGPPs form in the outer disk, as expected, at distances of about 8 AU. The disks were initially seeded with $m = 2$ perturbations, so the occurrence of two GGPPs may be an artifact of this assumption; in an unbiased disk, it may be that a single GGPP would form at a given radius. Forming two GGPPs at the same orbital distance might eventually result in a merger or in a close encounter, leaving both GGPPs with eccentric orbits.

Because of the strong growth of odd m modes, both models produce GGPPs with unequal masses. In model LI, one GGPP increased in mass from 4.5 to 6.2 M_J in the last 30 years, whereas the other GGPP decreased in mass from 1.3 to 0.36 M_J in the same time period. This trend suggests that the second GGPP might even disappear altogether at the expense of its more massive sibling. In model LA, a similar asymmetry results, with two GGPPs with masses of 7.8 and 3.7 M_J forming by 550 years and with the smaller GGPP losing mass as its sibling gains mass. The Jeans mass (26) is about 0.2 M_J for model LI and 1.2 M_J for model LA; because of the adiabatic assumption, the GGPPs have $T \approx 300$ K in the latter case and $T \approx 100$ K in the former. The larger mass GGPPs are above the Jeans mass and so are gravitationally bound, but the smaller mass GGPPs may not survive. The larger GGPPs also are stable with respect to tidal disruption by the gravitational force of the central protostar; at an orbital distance of 8 AU, the critical tidal radius or inner Lagrangian point (27) is about 1 AU from the center of the GGPPs, which is slightly larger than the radius of the GGPPs in the radial direction.

Model LA shows that a GGPP can form in a moderately massive ($\sim 140 M_J$) disk even if the perturbation behaves adiabatically, that is, even if the GGPP is unable to cool by radiation during its growth phase. Coupled with the GGPP formation in model LI, it appears that GGPP formation can occur in protoplanetary disks regardless of the exact thermodynamics of the instability.

Because only two models are presented here, the final masses and distances of these GGPPs should be considered only as rough

indicators of the type of outcome to be expected. The intent here is not to try to match the characteristics of any specific giant planet but merely to demonstrate the feasibility of the gravitational instability theory of their formation.

Although the long-term evolution of marginally unstable disks is uncertain (19), the GGPP instability is likely to occur if a means exists for suddenly driving Q below 1. Clumpy accretion of molecular cloud gas by the disk may be sufficient to increase the disk's surface mass density, driving $Q < 1$ over a short time scale and triggering the GGPP instability in a marginally stable disk. Observations of infalling gas in the B335 protostellar system (28) reveal the presence of 0.01 pc-sized, multiple- M_J clumps that may lead to episodic disk accretion. These non-self-gravitating clumps will be focused by the converging trajectories of the collapsing gas and will impact an annulus of the disk. A focused clump with a length of 0.01 pc, moving at 14 km/s (infall velocity at 10 AU), will enter the disk within 600 years, which is possibly quick enough to trigger the GGPP instability.

With solar composition, a 1 M_J GGPP contains about 6 M_{\oplus} of elements heavier than H and He. If this ice and rock material exists in the form of dust grains, it could settle to the center of the GGPP and form an ice and rock core with a mass in the middle of the range presently inferred for Jupiter (3 to 10 M_{\oplus}). After the phase of evolution depicted in the present models, the GGPP should slowly contract for a period of $\sim 10^5$ years (18) before central temperatures become high enough (about 1000 K) to vaporize rocky dust grains or for water to become soluble in hydrogen (29). While the GGPP's gas is supported against collapse by the gas pressure gradient during this phase, the dust grains can grow by collisional coagulation and sediment down toward the center of the GGPP. Use of the same formalism used to model the coagulation and sedimentation of dust grains to the midplane of the solar nebula (30) produces a dust growth time (time for growth by a factor of $e \approx 2.7$) on the order of 10 years. Centimeter-sized grains could then coagulate in about 100 years, and these would sediment to the center of the GGPP within about 1000 years. Because these time estimates are shorter than the 10^5 years the GGPP requires to heat up enough to dissociate its molecular hydrogen and undergo a collapse to planetary densities, it appears that a substantial ice and rock core should form in a GGPP, with a mass determined by the initial metal abundance.

The new giant planet models (15) have global metal abundances that are in agree-

ment with those inferred from atmospheric observations: $Z = 0.02$ to 0.06 for Jupiter and $Z = 0.04$ to 0.12 for Saturn. The solar abundance is $Z = 0.02$, which implies that at least Saturn has a substantially nonsolar abundance. However, the presence of a radiative zone in the outermost layers (15) implies a barrier to whole planet mixing, so that atmospheric abundances may not apply to the entire planet. In addition, because of the uncertainties in the hydrogen equation of state at high pressure (15), future work might well yield global models that are even closer to solar composition. In any case, nonsolar envelope abundances will result from subsequent accretion of planetesimals in both the core accretion (7) and GGPP scenarios—Comet Shoemaker-Levy 9 was a striking example.

REFERENCES AND NOTES

1. M. Mayor and D. Queloz, *Nature* **378**, 355 (1995).
2. R. P. Butler and G. W. Marcy, *Astrophys. J.* **464**, L153 (1996).
3. G. Gatewood, *Bull. Am. Astron. Soc.* **28**, 885 (1996).
4. W. D. Cochran, A. P. Hatzes, R. P. Butler, G. W. Marcy, *ibid.*, p. 1111.
5. R. P. Butler, G. W. Marcy, E. Williams, H. Hauser, P. Shirts, *Astrophys. J.* **474**, L115 (1997).
6. J. B. Pollack, *Annu. Rev. Astron. Astrophys.* **22**, 389 (1984).
7. J. J. Lissauer, *Icarus* **69**, 249 (1987); J. B. Pollack *et al.*, *ibid.* **124**, 62 (1996). These studies assumed a higher than normal surface mass density in the disk, the maximum possible gravitational enhancement factor, and an infinite reservoir of disk gas; assumptions that probably are not all warranted. Even with these favorable assumptions, S. J. Weidenschilling [*Lunar Planet. Sci. Conf. XXVIII*, 1513 (1997)] found that runaway accretion would stall and produce only 2 to 3 M_{\oplus} cores.
8. S. E. Strom, S. Edwards, M. F. Skrutskie, in *Protostars & Planets III*, E. H. Levy and J. I. Lunine, Eds. (Univ. of Arizona Press, Tucson, 1993), pp. 837–866.
9. G. W. Wetherill, in *Planetary Systems: Formation, Evolution, and Detection*, B. F. Burke, J. H. Rahe, E. E. Roettger, Eds. (Kluwer, Dordrecht, Netherlands, 1994), pp. 23–32; G. A. H. Walker *et al.*, *Icarus* **116**, 359 (1995).
10. D. N. C. Lin and J. Papaloizou, *Mon. Not. R. Astron. Soc.* **191**, 37 (1980).
11. D. W. Latham, T. Mazeh, R. P. Stefanik, M. Mayor, G. Burki, *Nature* **339**, 38 (1989).
12. G. W. Marcy and R. P. Butler, *Astrophys. J.* **464**, L147 (1996).
13. A. P. Boss, *Nature* **379**, 397 (1996); *Phys. Today* **49** (no. 9), 32 (1996).
14. H. Mizuno, *Progr. Theor. Phys.* **64**, 544 (1980).
15. G. Chabrier, D. Saumon, W. B. Hubbard, J. I. Lunine, *Astrophys. J.* **391**, 817 (1992); T. Guillot, G. Chabrier, P. Morel, D. Gautier, *Icarus* **112**, 354 (1994).
16. D. J. Stevenson, *Planet. Space Sci.* **30**, 755 (1982).
17. G. P. Kuiper, *Proc. Natl. Acad. Sci. U.S.A.* **37**, 1 (1951); A. G. W. Cameron, *Moon Planets* **18**, 5 (1978).
18. P. Bodenheimer, A. S. Grossman, W. M. DeCampi, G. Marcy, J. B. Pollack, *Icarus* **41**, 293 (1980).
19. G. Laughlin and P. Bodenheimer, *Astrophys. J.* **436**, 335 (1994).
20. P. M. Cassen, B. F. Smith, R. H. Miller, R. T. Reynolds, *Icarus* **48**, 377 (1981).
21. A. P. Boss, *Astrophys. J.* **469**, 906 (1996). Unlike viscous accretion disk models, in which viscous

- dissipation provides the heating source, the temperatures in these models are derived from a balance between radiative losses and compressional heating caused by gas infalling onto the disk and moving inward toward the protostar. The disks have a surface density profile $\sigma \propto r^{-1/2}$ (from 1 to 10 AU) chosen to ensure Keplerian rotation.
22. For an axisymmetric, thin, collisionless disk, A. Toomre [*Astrophys. J.* **139**, 1217 (1964)] showed that a nonaxisymmetric perturbation will be unstable if $Q < 1$. Values of $Q \approx 1$ imply either marginal stability or instability. For a disk in Keplerian rotation, as is approximately the case here, Q is defined as $Q = 0.936c_s\Omega/\pi G\sigma$, where c_s is the sound speed, Ω is the disk rotation rate, G is the gravitational constant, and σ is the surface (mass) density of the disk. For locally adiabatic variations in the disk temperature, the sound speed is defined as $c_s = (\gamma p/\rho)^{1/2}$.
 23. G. W. Wetherill, *Annu. Rev. Earth Planet. Sci.* **18**, 205 (1990); *Icarus* **119**, 219 (1996).
 24. A. P. Boss and E. A. Myhill, *Astrophys. J. Suppl. Ser.* **83**, 311 (1992).
 25. A. P. Boss, *Lunar Planet. Sci. Conf.*, in press.
 26. The Jeans mass is the mass of a sphere of uniform density gas with a radius equal to the Jeans length. The Jeans length is the critical wavelength necessary for self-gravitational collapse of an isothermal medium [L. Spitzer, *Diffuse Matter in Space* (Interscience, New York, 1968), p. 216]. In cgs units, the Jeans mass is given by $1.3 \times 10^{23} (T/\mu)^{3/2} \rho^{-1/2}$, where μ is the mean molecular weight.
 27. The Lagrangian points define the region within which matter can be considered to be gravitationally bound to a planet in orbit about a star. The critical tidal radius is calculated by W. M. DeCampi and A. G. W. Cameron, *Icarus*, **38**, 367 (1979).
 28. T. Velusamy, T. B. H. Kuiper, W. D. Langer, *Astrophys. J.* **451**, L75 (1995).
 29. D. J. Stevenson and E. Fishbein, *Lun. Planet. Sci. Conf. XII* 1040 (1981).
 30. S. J. Weidenschilling, in *Meteorites and the Early Solar System*, J. F. Kerridge and M. S. Matthews, Eds. (Univ. of Arizona Press, Tucson, 1988), pp. 348–371.
 31. I thank S. Peale, G. Wetherill, and an anonymous referee for improvements to the manuscript. Supported in part by the Planetary Geology and Geophysics Program of NASA under grant NAG5-3873. Calculations were performed on the DEC Alpha workstations of the Carnegie Institution of Washington.

8 April 1997; accepted 7 May 1997

Oxygen on Ganymede: Laboratory Studies

R. A. Vidal,* D. Bahr, R. A. Baragiola,† M. Peters

To test proposals for the origin of oxygen absorption bands in the visible reflectance spectrum of Ganymede, the reflectance of condensed films of pure oxygen (O₂) and O₂-water mixtures and the evolution of O₂ from the films as a function of temperature were determined. Absorption band shapes and positions for oxygen at 26 kelvin were similar to those reported for Ganymede, whereas those for the mixtures were slightly shifted. The band intensity dropped by more than two orders of magnitude when the ice mixture was warmed to 100 kelvin, although about 20 percent of the O₂ remained trapped in the ice, which suggested that at these temperatures O₂ molecules dissolve in the ice rather than aggregate in clusters or bubbles. The experiments suggest that the absorption bands in Ganymede's spectrum were not produced in the relatively warm surface of the satellite but in a much colder source. Solid O₂ may exist in a cold subsurface layer or in an atmospheric haze.

Recent optical reflectance measurements of Ganymede revealed the presence of oxygen. Spencer *et al.* (1) found two weak absorption bands in the visible (at 5773 and 6275 Å) spectrum of Ganymede (but not of other icy satellites) that are signatures of interacting pairs of O₂ molecules (double transitions in adjacent molecules). In addition, Noll *et al.* (2) found a strong absorption band in the near ultraviolet (UV), which suggested the presence of condensed ozone. These oxygen signatures were prominent on Ganymede's trailing side, the side that is more subject to bombardment by ions from Jupiter's magnetosphere. This hemispherical difference led to suggestions that oxygen or ozone molecules originate either from direct implantation of oxygen ions into the surface or from radiolysis of ice, which accumulates beneath the surface

(1–3). However, the oxygen features were not seen in Europa's spectrum even though it is more heavily bombarded with ions and has been thought to have a denser oxygen atmosphere (4).

Ganymede's band positions were close to those previously measured for solid oxygen (5). To determine whether similar band positions result from condensed oxygen embedded in ice or other materials that may be present on Ganymede's surface, we measured optical reflectance spectra of pure solid oxygen, condensed O₂-H₂O mixtures, and irradiated ice. The experiments were made in a cryopumped ultrahigh-vacuum chamber (with a base pressure of $\sim 10^{-10}$ torr). We grew condensed gas films at ~ 13 Å/s by dosing degassed, pure water vapor or a 1:1 O₂-H₂O mixture onto the optically flat gold surface of a cooled quartz crystal microbalance. A quadrupole mass spectrometer measured the gas evolving from the films as they warmed up. The bidirectional reflectance was measured at a 90° phase angle and divided by the reflectance of a pure water ice film to remove the shape of the lamp spectrum and spectrometer efficiency function (6, 7).

The reflectance spectra of Ganymede

(1) are compared with the spectra of pure oxygen taken at the growth temperature 26 K (Fig. 1) (the films disappear in seconds if heated above 33 K). The absorption spectra, normalized for each band, obtained from Fig. 1 after the subtraction of the smooth continuum baselines are shown in Fig. 2. The position and shape of the bands for pure oxygen are similar to those observed on Ganymede and similar to those obtained in transmission experiments (5) for β -oxygen but are slightly shifted. To make a quantitative comparison, we estimated the optical path length L in our films as 2.4 times the film thickness, considering only single scattering events in the film and specular reflection at the substrate, because both absorption and scattering were weak. We obtained the absorption coefficient $\alpha(\lambda)$ at a wavelength λ from the decrease in reflectance $R(\lambda)$ due to absorption $R(\lambda) = 1 - \exp[-L\alpha(\lambda)]$. The integrated absorption coefficients $A = \int \alpha(\lambda)d\lambda$, given in Table 1 in mass units, agreed with previous reports (5) that used a density of 1.4 g/cm³.

Spencer *et al.* (1) suggested that the oxygen on Ganymede is trapped in the ice, because at the minimum recorded daytime temperature on Ganymede, oxygen is liquid or gaseous with a vapor pressure (~ 75 mbar) that is orders of magnitude larger than the surface pressure upper limit implied by stellar occultation experiments (8, 9). Oxygen from a tenuous atmosphere could slowly accumulate in Ganymede's surface ice. Although it is known that microporous amorphous ice can trap gases efficiently below 110 K (10), the state of the trapped gas is not known; it can be in the form of gas bubbles in micropores or it may become dispersed into forms such as clathrate hydrates (11). This question can be addressed by looking at the optical bands due to O₂ pairs because their absorption strength depends on intermolecular distance (12).

We exposed a 17- μ m-thick amorphous H₂O ice film to a flow of O₂ for 16 hours at

R. A. Vidal, D. Bahr, R. A. Baragiola, Laboratory for Atomic and Surface Physics, University of Virginia, Thornton Hall, Charlottesville, VA 22901, USA.

M. Peters, School of Medicine, Laboratory of Physics, Teikyo University, Ohtsuka 359, Hachioji-shi, Tokyo 192, Japan.

*Present address: Instituto de Tecnología Quíonica, Güemes 3450, 3000 Santa Fé, Argentina.

†To whom correspondence should be addressed. E-mail: raul@virginia.edu